

Interlayer Link Prediction in Multiplex Social Networks Based on Multiple Types of Consistency between Embedding Vectors

Rui Tang¹, Zhenxiong Miao¹, Shuyu Jiang¹, Xingshu Chen^{1,2*}, Haizhou Wang^{1,2*}, Wenxian Wang², Mingyong Yin³, and Wei Wang²

1. College of Cybersecurity, Sichuan University, Chengdu 610065, China

2. Cybersecurity Research Institute, Sichuan University, Chengdu 610065, China

3. College of Computer Science, Sichuan University, Chengdu 610065, China.

Abstract

Online users are typically active on multiple social media networks (SMNs), which constitute a multiplex social network. With improvements in cybersecurity awareness, users increasingly choose different usernames and provide different profiles on different SMNs. Thus, it is becoming increasingly challenging to determine whether given accounts on different SMNs belong to the same user; this can be expressed as an interlayer link prediction problem in a multiplex network. To address the challenge of predicting interlayer links, feature or structure information is leveraged. Existing methods that use network embedding techniques to address this problem focus on learning a mapping function to unify all nodes into a common latent representation space for prediction; positional relationships between unmatched nodes and their common matched neighbors (CMNs) are not utilized. Furthermore, the layers are often modeled as unweighted graphs, ignoring the strengths of the relationships between nodes. To address these limitations, we propose a framework based on multiple types of consistency between embedding vectors (MulCEV). In MulCEV, the traditional embedding-based method is applied to obtain the degree of consistency between the vectors representing the unmatched nodes, and a proposed distance consistency index based on the positions of nodes in each latent space provides additional clues for

*Corresponding Author: chenxsh@scu.edu.cn, whzh.nc@scu.edu.cn

prediction. By associating these two types of consistency, the effective information in the latent spaces is fully utilized. Additionally, MulCEV models the layers as weighted graphs to obtain better representation. In this way, the higher the strength of the relationship between nodes, the more similar their embedding vectors in the latent representation space will be. The results of our experiments on several real-world datasets demonstrate that the proposed MulCEV framework markedly outperforms current embedding-based methods, especially when the number of training iterations is small.

Keywords: social media network, interlayer link prediction, network embedding, multiplex network

1. Introduction

Social media network (SMN) applications have significantly enriched the daily lives of users and have attracted the attention of many researchers [1, 2, 3]. Most modern people leverage them for connection with one another, content sharing, and entertainment. According to a report by the Pew Research Center, 72% of U.S. citizens used some type of SMN in 2019 [4]. The situation is similar in China, which has 896 million SMN users [5]. To satisfy their diverse needs and interests, online users often make use of several SMNs simultaneously, for example by recording individual impressions of current events on Twitter, sharing photographs on Instagram, and searching for job information on LinkedIn. These various SMNs thus form a multiplex social network [6, 7, 8, 9, 10], of which each SMN constitutes a layer. Accounts are represented as nodes, and interactions within an SMN are represented as intralayer links in the multiplex network. If two accounts in different SMNs belong to the same user, an interlayer link exists between the corresponding nodes across different layers. The structure of a multiplex network has a significant influence on cascades [11], propagation [12], synchronization [13], and games [14].

The goal of interlayer link prediction is to leverage feature or structure information to determine whether accounts across different SMNs belong to the same user [15]; this is a challenging task in multiplex network analysis. It is also known as anchor link prediction [16, 17], network alignment [18, 19, 20, 21, 22], user identification [23], and user identity linkage [21].

As hacking attempts have become more frequent, online users' security awareness has gradually increased. An increasing number of users create ac-

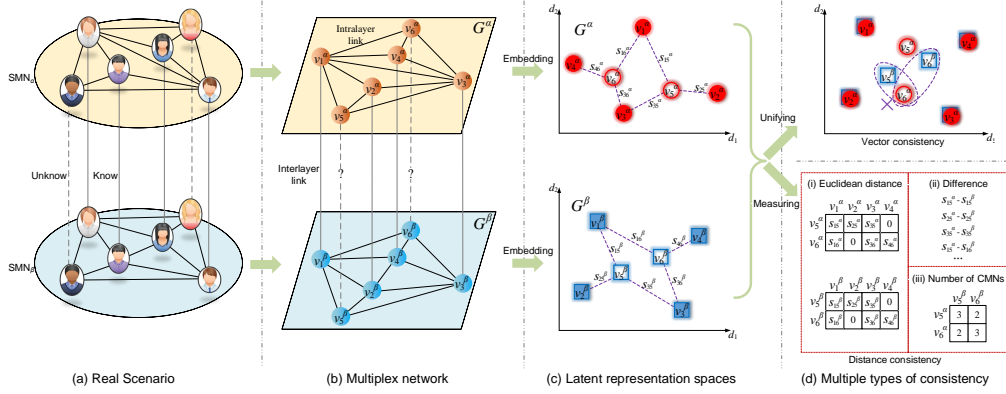


Figure 1: Example of interlayer link prediction based on multiple types of consistency between embedding vectors. (a) Real scenario: There are two SMNs, each of which has six user accounts. The accounts linked by the vertical gray line belong to the same user. The correspondence of the account pairs linked by a solid gray line is known in advance; the task is to determine the correspondence of the other accounts. (b) Multiplex network: The multiple SMNs are represented by a multiplex network. The task of determining whether accounts on different SMNs belong to the same user becomes the task of predicting the unobserved interlayer links in the multiplex network. (c) Latent representation spaces: Network embedding techniques are used to address the interlayer link prediction problem. Each layer of the multiplex network is embedded into a latent representation space. (d) Multiple types of consistency: The degree of match to estimate whether an interlayer link exists between two unmatched nodes across different layers consists of two parts. One is the degree of vector consistency (upper part), and the other is the degree of distance consistency (lower part).

counts under different usernames, hide profile information, or even provide fake content on profile configuration pages [24]. In this way, users access SMNs anonymously to make friends, share information, and discuss problems, thereby not only using multiple SMNs simultaneously but also protecting their privacy. However, such anonymity can pose a certain degree of harm to society. Cybercriminals register a large number of accounts on multiple SMNs and subsequently engage in various types of illegal activities. For example, they might circulate messages containing untruths, spread malware program links, or initiate financial fraud on these SMNs [25]. Predicting the interlayer links of the multiplex network comprising different SMNs can help criminal investigation authorities establish cybercriminals' patterns of law violations, model their online behaviors, identify their regions of activity, or even determine their real-world identities, thereby effectively fighting cybercrime.

There are other benefits as well to predicting the interlayer links in a multiplex network. For instance, because information and rumors typically spread across multiple SMNs, predicting interlayer links can help improve the understanding of information diffusion [26]. Furthermore, the use of SMNs as evidence in trials related to issues of custody, divorce, and insurance is rising rapidly [27]. A method for identifying the interlayer links across multiple SMNs would be a powerful tool in the collection of evidence for civil and criminal investigations.

The problem of predicting interlayer links in a multiplex network is typically solved by leveraging feature or structure information accessed from the multiple SMNs. Currently, there are three main approaches for handling this problem: (i) feature-based prediction, (ii) network-based prediction, and (iii) a combination of multiple approaches. Of these, network-based methods have attracted more attention; they show increasing promise because few people share the same circle of friends [28], and information on connections in SMNs is quite easy to obtain [29].

In recent years, network embedding techniques have been utilized to learn latent, low-dimensional representations of network nodes while preserving network structure. After all of the nodes are represented as low-dimensional vectors into the latent representation space, advanced network analytic tasks such as node classification, community detection, and link prediction can be efficiently carried out. [30]. Motivated by the advances in network embedding techniques for single-network tasks, researchers have proposed several strategies to leverage these techniques for solving the interlayer link prediction problem [31, 32, 33]. Typically in these studies, network embedding techniques are used first, to learn the latent representations of nodes in different layers of the multiplex network. After that, a priori interlayer node pairs are constrained to have the same latent representations to unify nodes into a common latent representation space. Finally, the unobserved interlayer links are predicted by comparing the embedding vectors of unmatched nodes across different layers in the common latent space.

To unify all nodes into a common latent space and predict the unobserved interlayer links, most embedding-based methods utilize a priori interlayer links to train an approximate mapping function after achieving the latent representations, as was done in Refs. [34, 31, 33, 35]. However, the perfect mapping function is difficult to obtain, as each layer’s latent space is unknown to the others [33], and this leads to unsatisfactory performance, especially when the number of training iterations is small. Apart from pre-

dicting the unobserved interlayer links by comparing the embedding vectors in the common latent space unified by the mapping function, the positional relationship between unmatched nodes and their common matched neighbors (CMNs) can also be used to measure whether an interlayer link exists between two unmatched nodes that lie in different layers. In other words, the effective information in the latent representation spaces is not fully utilized.

Figure 1 illustrates the general components of interlayer link prediction based on multiple types of consistency between embedding vectors. As shown in the top half of Fig. 1(d), if we use only the information in the common latent space unified by the mapping function, the node v_6^α will be matched with \mathbf{v}_5^β as their embedding vectors are more consistent. However, if we analyze the positional relationship between unmatched nodes and their CMNs simultaneously, we might uncover more clues for predicting the unobserved interlayer links. We propose a “distance consistency” index to measure this relationship. As shown in the lower half of Fig. 1(d), three aspects are considered in the distance consistency index: (i) the Euclidean distance between the unmatched node and its matched neighbor, (ii) the difference between two Euclidean distances formed by unmatched nodes across different layers and their CMNs, and (iii) the number of CMNs.

When each layer of the multiplex network is embedded into a latent representation space, different layers are often modeled as unweighted graphs, and the strength of the relationships between nodes is often ignored. However, the intralayer links between nodes may have different relationship strengths. For example, if a boy has only one friend, the friendship between him and his friend is highly likely to be closer than one between individuals who have many friends. To distinguish among relationship strengths, the intralayer links between nodes should be weighted. To address this problem, we propose a weighted-embedding method to embed each layer of the multiplex network in the form of weighted graphs based solely on the network structure.

In this study, we developed a framework based on multiple types of consistency between embedding vectors (MulCEV) for interlayer link prediction in a multiplex network; it focuses on making full use of information in the latent representation spaces for prediction and on modeling different layers as weighted graphs to obtain better representation. The main contributions can be summarized as follows:

- We propose a distance consistency index that is based on the positions

of nodes in each latent representation space, which leverages CMNs of the unmatched nodes across different layers as references to provide additional clues for predicting interlayer links. The degree of match to estimate whether an interlayer link exists between two unmatched nodes across different layers consists of two parts: the degree of vector consistency, which applies the traditional embedding-based method to measure the consistency of the embedding vectors of the unmatched nodes in the common latent representation space, and the degree of distance consistency proposed above. The effective information in the latent representation spaces is fully utilized by associating these two types of consistency between embedding vectors.

- We model each layer of the multiplex network as a weighted graph to obtain better representation based solely on the network structure. Thus, the higher the strength of the relationship between nodes, the closer are their embedding vectors in the latent representation space.
- In order to reduce the time complexity, we adopt the technique of matrix multiplication to optimize the process of calculating the distance consistency and vector consistency for all unmatched node pairs.
- We test the effectiveness of the proposed MulCEV framework on two widely used real-world multiplex networks and report the results against those of state-of-the-art methods.

The rest of this paper is organized as follows. Section II systematically reviews related work. Section III presents preliminaries and problem definitions. Section IV describes the MulCEV framework in detail. Section V presents details of the datasets used in the experiments, comparison methods, and the experimental results. Finally, Section VI concludes the paper and proposes areas for future research.

2. Related Work

The problem of interlayer link prediction in the multiplex network is typically solved by leveraging feature or structure information accessed from the multiple SMNs [3]. Early studies focused on feature information; they analyzed user profiles, location trajectories, and user-generated content to link nodes across different SMNs belonging to the same user. Profile features

included username, image, position, birthday, job, and experience, among others [36]. The authors of Refs. [37, 38, 39, 40, 41] explored ways of using usernames for prediction. References [42, 43, 44, 45, 46, 34] considered various profile attributes to improve prediction performance. With the rapid development of SMNs, many users began using different usernames in different SMNs for security reasons. Meanwhile, the accessible profile information among SMNs became increasingly fragmented, unavailable, and disruptive [29]. These SMN characteristics marginalized the traditional profile-based resolutions. The trajectory-based method has been popular since the emergence of the mobile-phone-based Internet. SMN users who wish to announce their location to their friends on some SMN applications can tap a “check-in” button to see a list of nearby places and choose the place that matches their location. References [47, 48, 49] focused on these check-in data and used them to link identities. Such trajectory-based methods, however, often face data sparsity problems, and users usually share different locations on different SMNs. User-generated content can reveal some unique characteristics of an SMN user, such as his or her writing style [50, 51] or footprint [52]. These methods rely heavily on the availability of excellent natural language processing (NLP) techniques and text preprocessing algorithms because user-generated content often includes spoken words, emotion icons, and abbreviations.

Data on a network’s structure are highly accessible and difficult to counterfeit. In addition, a user’s friend circle is highly personalized; i.e., few people share the same friend circle [28]. Therefore, network-based methods are an ideal solution for the interlayer link prediction problem and have attracted the interest of an increasing number of researchers in recent years. Network-based methods can be divided into non-embedding-based methods and embedding-based methods according to whether network embedding techniques are used.

2.1. Non-embedding-based Methods

Given the completeness and connectivity of a network structure, two kinds of structural information can be used to solve the interlayer link prediction problem. The first is local network information, which focuses on the one-hop neighborhood (e.g., follower/followee/friend relationships) of the unmatched nodes [3]. Narayanan and Shmatikov proposed a re-identification algorithm, which was the first method to use a graph-theoretic model based on the node neighborhood to solve this problem [53]. Later, Korula et al. [54] computed

a similarity score for an unmatched node pair by counting the number of CMNs and then keeping all the links above a specific threshold. To avoid the possible problem of mismatching low-degree nodes in the early phases, only nodes whose degree is higher than a specified threshold are allowed to be matched. Zhou et al. [28] proposed a friend-relationship-based user identification (FRUI) algorithm that counts the number of shared friends to calculate the degree of match for all candidate-matched node pairs and chooses pairs that have the maximum value as the final set of matched pairs. Tang et al. [15] further investigated the importance of the scale-free property of real-world SMNs for accomplishing interlayer link prediction and proposed a degree penalty principle to calculate the degree of match of all unmatched node pairs. Ren et al. [55] defined a set of meta-diagrams for feature extraction and used greedy link selection for the interlayer link prediction.

The second type of structural information is global network information. Zhu et al. [56] transformed the interlayer link prediction problem into a maximum common subgraph problem and maximized the number of intralayer links to obtain a cross-layer mapping. Zafarani and Liu [23] also explored a solution utilizing global network information. They calculated the Laplacian matrices for each layer and used a matrix optimization method to perform the prediction.

The above methods were used mainly for dealing with the two-layer case, although most researchers suggested that their approaches could be extended to a three- or four-layer multiplex network. Other researchers have studied this case. The authors of Ref. [57] considered both local and global consistency to match nodes across more than two layers: local consistency for matching nodes across just two layers, and global consistency for dealing with the cases involving more than two layers. In Ref. [58], an algorithm is proposed to resolve the one-to-one constraint in the situation of cross-multiple layers. This algorithm matches nodes by minimizing the friendship inconsistency and selects the node pairs; it can lead to the maximum confidence scores for the multiplex network.

Other scholars have studied the interlayer link prediction problem from a different perspective. Zhang et al. [59] proposed a joint link fusion algorithm to predict the intralayer links and interlayer links simultaneously. In Refs. [60, 61], the authors studied ways of predicting interlayer links in the absence of a priori interlayer links.

2.2. *Embedding-based Methods*

Network embedding techniques aim to represent nodes in a network by low-dimensional vectors in a latent representation space so that advanced analytic tasks, such as node classification, community detection, and link prediction, can be conducted more efficiently in both time and space [62]. DeepWalk [63] leverages uniform random walks to generate a set of node sequences that are similar to the word sequences in natural language and uses the skip-gram model to learn vertex representations of nodes. Node2vec [64] demonstrated that DeepWalk is not sufficiently expressive to capture a more global structure and incorporated a biased random walk strategy to improve it. Tang et al. [65] proposed a large-scale information network embedding (LINE) approach to preserve both the first- and second-order proximities between nodes. Subsequently, Wang et al. [66] preserved not only the first- and second-order proximity of vertices but also the community structure. There have been numerous other studies using network embedding techniques such as dynamic network embedding [67, 68] and embedding for scale-free networks [69].

Increasingly, computer and network scientists are exploring ways of employing network embedding techniques to improve their ability to predict interlayer links in terms of accuracy, applicability, and efficiency. Tan et al. [70] tried to map accounts across SMNs based on network embedding, adopting hypergraphing to model high-order relations of SMNs and representing nodes in a common latent space. Their method infers correspondence by comparing distances between the vectors of the unmatched nodes. Liu et al. [32] represented the multiple SMNs with a shared latent space and determined the interlayer links by computing the cosine similarity between the latent space vector of one node in layer α and another in layer β . The network embedding process was integrated with the entity alignment process under a unified optimization framework. They further refined their proposed method in Ref. [71] by incorporating structural diversity. The structural diversity focuses on the impact of whether the a priori matched nodes come from different communities.

Instead of embedding all layers into a common latent space, Man et al. [31] projected each SMN into a unique latent space and represented nodes by low-dimensional vectors in the latent space. Then, they trained a cross-layer mapping function for predicting interlayer links. Zhou et al. [33] adopted the same idea and proposed a semi-supervised approach that leverages dual learning to pretrain the mapping function to improve prediction accuracy.

They focused on learning latent semantics of both the node representation and the network structure [22]. Zhou et al. [72] studied the scenario without a priori interlayer links and proposed an unsupervised approach for the prediction. Considering time complexity, Wang et al. [35] proposed a framework that directly learns a binary hash code for each node across SMNs, which obtained high time efficiency while maintaining competitive prediction accuracy. In Ref. [17], the authors adopted active learning to reduce the cost of labeling a priori node pairs. In Ref. [20], the authors viewed all of the nodes in one layer as a whole and executed the prediction at the distribution level. Chu et al. [19] considered multi-layer scenarios in which the number of layers is more than two. They refined two types of low-dimensional vectors for each node: an inter-vector for interlayer link prediction, and an intra-vector for downstream network analysis tasks.

In some studies, structural information and attribute information were embedded simultaneously to perform the interlayer link prediction. Wang et al. [73] proposed a linked heterogeneous network embedding (LHNE) method to fuse the content and structural information of a user into a unified latent representation space to identify account linkages. In Ref. [74], the authors proposed a semi-supervised network embedding method to learn the attribute information and structural information simultaneously. Heterogeneous SMNs differ substantially in several aspects, including network structure, user behavior, and user information. TransLink [21] captures the heterogeneities of SMNs and embeds both nodes and their various types of interactions into a unified latent space.

3. Preliminaries and Problem Statement

Table 1 displays the main symbols and notation used in this paper. We follow the common symbolic conventions, wherein bold uppercase letters denote matrices, bold lowercase letters denote column vectors, and lowercase letters denote scalars.

3.1. Definitions

In general, an SMN can be represented as a graph $G(V, E)$, where V is a node set representing all the accounts in the SMN, and $E \subseteq V \times V$ is an edge set representing the relationships among the accounts. Multiple SMNs can constitute a multiplex network.

Table 1: Symbols and notations

Symbol	Description
\mathcal{M}	The multiplex network.
G	A SMN which is one layer of \mathcal{M} .
u, v	Nodes in \mathcal{M} .
\mathbf{u}, \mathbf{v}	Embedding vectors of nodes u and v respectively.
α, β	Layer indices of \mathcal{M} .
e^α, e^β	Intralayer links in G^α and G^β respectively.
\mathbf{e}, \mathbf{E}	Intralayer links vector and intralayer link matrix respectively.
$e^{\alpha\beta}$	Interlayer link.
i, j, a, b	Node indices.
n^α, n^β	Number of nodes in G^α and G^β .
n, m	Number of a priori interlayer links and unobserved interlayer links respectively.
$\Gamma(v_i)$	Set of neighbors of node v_i .
k_v	Degree of node v
p, \mathbf{P}	Degree of vector consistency and Degree of vector consistency matrix respectively.
q, \mathbf{Q}	Degree of distance consistency and Degree of distance consistency matrix respectively.
r, \mathbf{R}	Degree of match and Degree of match matrix respectively.
d	Dimensionality of the latent representation space.
ϕ	Mapping function.
w	weight of the intralayer link.
δ	control parameter.
Φ	Set of a priori interlayer links.
Ψ	Set of unobserved interlayer links.

Definition 1: Multiplex network. Given a set of SMNs, we can denote them using superscripts α, β, \dots , such as by $G^\alpha(V^\alpha, E^\alpha), G^\beta(V^\beta, E^\beta), \dots$. These multiple SMNs can be seen as a pair $\mathcal{M} = (g, c)$, where $g = \{G^\alpha | \alpha \in \{1, \dots, m\}\}$ is a family of graphs denoting the different SMNs and

$$c = \{E^{\alpha\beta} \subseteq V^\alpha \times V^\beta | \alpha, \beta \in \{1, \dots, m\}, \alpha \neq \beta\} \quad (1)$$

is the set of interconnections between the nodes of G^α and G^β , where $\alpha \neq \beta$. Each element in g is referred to as a layer in multiplex network \mathcal{M} . The elements of E^α are referred to as intralayer links, and the elements of $E^{\alpha\beta}$ are called interlayer links. The interlayer links are also called interlayer node pairs, and the nodes belonging to these pairs can be called interlayer nodes. The interlayer links that are given in advance are called a priori interlayer links or a priori interlayer node pairs, and the other interlayer links are called unobserved interlayer links. The nodes belonging to the a priori interlayer node pairs are called matched nodes, and the other nodes are called unmatched nodes. A node pair consisting of two unmatched nodes across different layers can be called an unmatched node pair.

Definition 2: Common matched neighbor (CMN). Given an a priori interlayer node pair (v_i^α, v_j^β) , a node v_a^α in layer α , and a node v_b^β in layer β , if an intralayer link exists between v_a^α and v_i^α and another interlayer link exists between v_b^β and v_j^β , we can say that the a priori interlayer node pair (v_i^α, v_j^β) is the CMN of nodes v_a^α and v_b^β .

Definition 3: Network embedding model. Given a layer $G^\alpha(V^\alpha, E^\alpha)$ of the multiplex network \mathcal{M} , a network embedding model learns to represent each node $v_i^\alpha \in V^\alpha$ as a low-dimensional vector $\mathbf{v}_i^\alpha \in \mathbb{R}^d$, where d represents the dimensionality of the latent representation space.

Definition 4: Mapping function. In the method proposed in this paper, each layer is embedded into a single latent representation space. Given a set of interlayer links, the function ϕ is defined as a mapping from layer α to layer β such that for each interlayer node pair (v_i^α, v_j^β) , we have $\phi(\mathbf{v}_i^\alpha) = \mathbf{v}_j^\beta$.

Generally, the perfect mapping function is hard to obtain, as each layer's latent space is unknown to the others [33]. Most embedding-based methods utilize a priori interlayer links to train an approximate mapping function after achieving the latent representations. After obtaining the approximate mapping function, the unmatched nodes can be unified in a common latent space by this function.

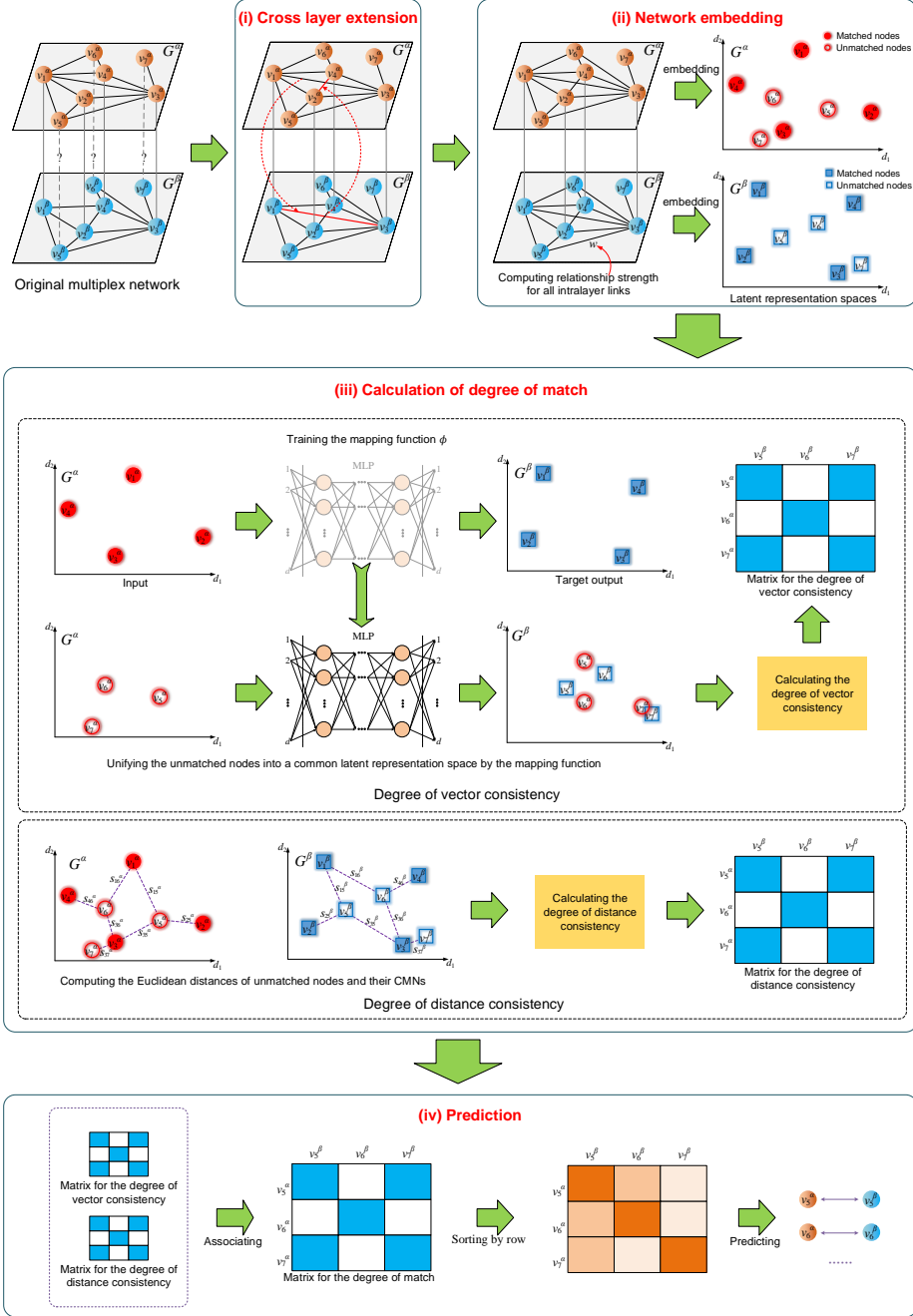


Figure 2: Overview of MulCEV.

3.2. Problem Statement

Supposing that we have a multiplex network \mathcal{M} with a set of a priori interlayer links, the interlayer link prediction problem is to determine whether any unmatched node pair v_i^α, v_j^β chosen from V^α and V^β have an interlayer link, i.e., whether the accounts represented by the two unmatched nodes belong to the same person.

Given an unmatched node pair (u_i^α, u_j^β) across different layers in the multiplex network \mathcal{M} , interlayer link prediction learns a binary function $f : V^\alpha \times V^\beta \rightarrow 0, 1$ such that

$$f(u_i^\alpha, u_j^\beta) = \begin{cases} 1, & \text{if } e_{ij}^{\alpha\beta} \text{ exist} \\ 0, & \text{otherwise} \end{cases}, \quad (2)$$

where $f(u_i^\alpha, u_j^\beta) = 1$ means that there is an interlayer link between unmatched nodes v_i^α and v_j^β .

It is worth noting that some people may register two or more accounts in a given SMN. For simplicity, we assume that these accounts belong to different individuals.

4. Proposed Framework

The proposed framework (shown in Fig. 2) is an algorithm consisting of four main components: (i) cross-layer extension, (ii) network embedding, (iii) calculation of the degree of match, and (iv) prediction. We discuss each one in detail in the following sections.

4.1. Cross-layer Extension

Given two nodes with an interlayer link in the multiplex network, it is usually true that they have an intralayer link in one layer if there exists a connection in the other layer [75]. The cross-layer extension is to leverage a priori interlayer links to extend the intralayer links in each layer of the multiplex network, as shown in Fig. 2 (i).

Given a multiplex network \mathcal{M} with two layers G^α and G^β , a priori interlayer link set Φ , and intralayer link sets E^α and E^β , the extended network \tilde{G}^α of layer α can be described as

$$\tilde{E}^\alpha = E^\alpha \cup \{(v_i^\alpha, v_j^\alpha) | (v_i^\alpha, v_a^\beta) \in \Phi, (v_j^\alpha, v_b^\beta) \in \Phi, (v_a^\beta, v_b^\beta) \in E^\beta\}, \quad (3)$$

referring to Ref. [31]. The extended network \tilde{G}^β of layer β is similar to the above equation. Note that it is not essential to perform cross-network extension.

4.2. Network Embedding

During network embedding, nodes that are “close” to each other in the network are embedded in such a way that they have similar vector representations [76]. How is it determined whether two nodes are “close”? Various scholars have proposed different methods. DeepWalk [63] leverages a truncated random walk to generate a set of node sequences for learning the representations. This method considers nodes with intralayer links to be close. LINE [65] uses the notion of first- and second-order proximities to measure closeness, where first-order proximity refers to intralayer links and second-order proximity refers to two nodes having common neighbors. These embedding methods often model different layers as unweighted graphs. However, different intralayer node pairs may have different relationship strengths. For example, if a boy has only one friend, the friendship between him and his companion is highly likely to be closer than that between those who have many friends. To distinguish between relationship strengths, the intralayer connection between nodes should be weighted. We propose a weighted-embedding method that embeds each layer of the multiplex network in the form of weighted graphs based purely on the network structure.

The strength of the relationship between two nodes in the same layer can usually be characterized by the number of neighbors they have in common. However, the number of intralayer links a node has also affects the strength of its relationship with other nodes, and the degrees of their common neighbors may also affect relationship strength. Considering these three factors, we propose the following formula:

$$w_{ij} = ((\sum_{z \in \Gamma(v_i) \cap \Gamma(v_j)} \frac{1}{\log k_z}) \cdot \frac{|\Gamma(v_i) \cap \Gamma(v_j)|}{|\Gamma(v_i) \cup \Gamma(v_j)|} + 1) \cdot e_{ij}, \quad (4)$$

where k_z is the degree of node z , and $\Gamma(\cdot)$ represents the neighbor set of node inside it.

Using the above formula has the following three advantages: (i) The greater the number of common neighbors between two nodes, the greater their weight; (ii) when two pairs of nodes have the same number of common neighbors, the node pair with fewer intralayer links will have the higher

weight; and (iii) the smaller the degree of the common neighbors between two nodes, the greater their weight.

After obtaining the weight of each intralayer link, we reference the network embedding model LINE [31] to update the node representation. For any intralayer link $e_{ij}^\alpha = (v_i^\alpha, v_j^\alpha)$ in a given layer α , the joint probability between node v_i^α and v_j^α is

$$z(v_i^\alpha, v_j^\alpha) = \frac{1}{1 + \exp(-(\mathbf{v}_i^\alpha)^\top \cdot \mathbf{v}_j^\alpha)}, \quad (5)$$

where \mathbf{v}_i^α and \mathbf{v}_j^α are the low-dimensional vectors of nodes v_i^α and v_j^α , respectively, which are defined in \mathbb{R}^d ; $z(\cdot, \cdot)$ is a distribution over the space $V^\alpha \times V^\alpha$, and $(\cdot)^\top$ is the transposition function. The empirical counterpart of $z(\cdot, \cdot)$ can be defined as $\hat{z}(\cdot, \cdot) = w_{ij}^\alpha / W$, where w_{ij}^α is the weight of the intralayer link e_{ij}^α as calculated by Eq. (4), and W is the summation of the weights of all intralayer links. By minimizing the KL-divergence [77] of $z(\cdot, \cdot)$ and its empirical counterpart $\hat{z}(\cdot, \cdot)$ over all the intralayer links in the α layer, the LINE model can be inferred. The objective function for embedding is

$$O = - \sum_{\forall (u_i^\alpha, u_j^\alpha) \in E^\alpha} \text{KL}(\hat{z}(u_i^\alpha, u_j^\alpha), z(u_i^\alpha, u_j^\alpha)), \quad (6)$$

where the KL-divergence $KL(\cdot, \cdot)$ is a method of measuring the similarity of two distributions. By omitting some constants, the objective function for embedding can be rewritten as

$$O = - \sum_{\forall (u_i^\alpha, u_j^\alpha) \in E^\alpha} w_{ij}^\alpha \log(z(u_i^\alpha, u_j^\alpha)). \quad (7)$$

By minimizing Eq. (7) over all the intralayer links independently, each of the nodes in the given layer α can be represented as a d -dimensional vector in the latent representation space with the stochastic gradient descent algorithm. The layer β of the multiplex network can be embedded by following the same steps.

4.3. Calculation of Degree of Match

For any two unmatched nodes across different layers, we calculate a score according to the MulCEV framework to estimate whether an interlayer link exists between them. We call this score the degree of match, which consists of two parts: the degree of vector consistency, and the degree of distance consistency. The details are as follows.

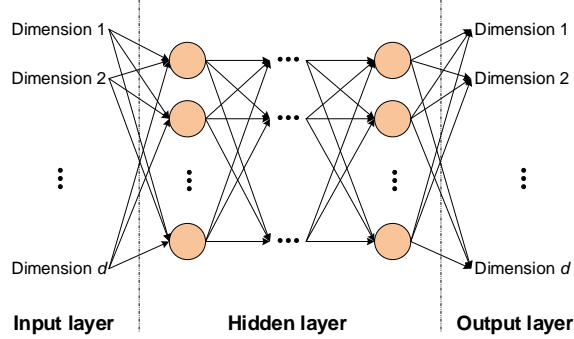


Figure 3: Structure of the multi-layer perceptrons (MLP). We used up to three hidden layers and up to 1200 neurons per layer. The numbers of neurons in the input layer and output layer depend on the dimensionality of the latent representation space.

4.3.1. Degree of vector consistency

We leverage the feed-forward multi-layer perceptrons (MLP) [78] to learn the mapping function from one layer to another based on the a priori inter-layer links. The structure of the MLP used in MulCEV is shown in Fig. 3. Given each of the a priori interlayer node pairs $(v_i^\alpha, v_j^\beta) \in E^{\alpha\beta}$ and their corresponding embedding vectors $(\mathbf{v}_i^\alpha, \mathbf{v}_j^\beta)$, we use \mathbf{v}_i^α as the input and \mathbf{v}_j^β as the target output to train the mapping function ϕ . The loss function of the MLP is

$$l(\mathbf{v}_i^\alpha, \mathbf{v}_j^\beta) = 1 - \cos(\phi(\mathbf{v}_i^\alpha), \mathbf{v}_j^\beta), \quad (8)$$

where $\cos(\cdot, \cdot)$ is the cosine similarity, and $\phi(\mathbf{v}_i^\alpha)$ is the actual output mapped by the MLP. The value of the loss function ranges from 0 to 2. Suppose that we have n a priori interlayer links; then for all a priori interlayer nodes, we use $\mathbf{A}^\alpha \in \mathbb{R}^{d \cdot n}$ and $\mathbf{A}^\beta \in \mathbb{R}^{d \cdot n}$ to represent their respective embedding vector matrices. The goal of training the MLP is to minimize the following cost function:

$$L(\mathbf{A}^\alpha, \mathbf{A}^\beta) = 1 - \cos(\phi(\mathbf{A}^\alpha), \mathbf{A}^\beta; \Theta), \quad (9)$$

where Θ is the collection of all parameters in the mapping function ϕ .

To obtain the degree of vector consistency, for any given unmatched node pair (u_a^α, u_b^β) with their embedding vectors \mathbf{u}_a^α and \mathbf{u}_b^β , we map node u_a^α into the latent representation space of the β layer according to the mapping function $\phi(\mathbf{u}_a^\alpha)$. We then use cosine similarity to compute the degree of vector

consistency between $\phi(\mathbf{u}_a^\alpha)$ and \mathbf{u}_b^β . The formula can be represented as

$$p(u_a^\alpha, u_b^\beta) = \frac{\phi(\mathbf{u}_a^\alpha)^\top \cdot \mathbf{u}_b^\beta}{\|\phi(\mathbf{u}_a^\alpha)\| \cdot \|\mathbf{u}_b^\beta\|}, \quad (10)$$

where $\|\cdot\|$ represents the 2-norm of the vector within.

4.3.2. Degree distance consistency

As shown in Fig. 1(d), if we consider only the degree of vector consistency, it may be difficult to obtain good prediction results in some cases, such as the incorrect match of (v_5^α, v_6^β) . The reason is that a perfect mapping function is difficult to obtain [33]. If we consider the positional relationship between the unmatched nodes and their matched neighbors in the embedding spaces of different layers, we might uncover additional clues for predicting the unobserved interlayer links. We propose a “distance consistency” index to measure this relationship, defined as

$$q(u_a^\alpha, u_b^\beta) = \sum_{\substack{\forall (v_i^\alpha, v_j^\beta) \in \Phi, \\ v_i^\alpha \in \Gamma(u_a^\alpha), \\ v_j^\beta \in \Gamma(u_b^\beta)}} \exp(-(s_{ai}^\alpha \cdot |s_{ai}^\alpha - s_{bj}^\beta| \cdot s_{bj}^\beta)). \quad (11)$$

In Eq. (11), Φ represents the set of a priori interlayer links, and s_{ai}^α is the Euclidean distance between unmatched node u_a^α and matched node v_i^α . The constraints in the equation indicate that the interlayer node pair (v_i^α, v_j^β) is the CMN of unmatched nodes u_a^α and u_b^β . Suppose that matched node pair (v_i^α, v_j^β) is the CMN of the unmatched nodes u_a^α and u_b^β ; then $|s_{ai}^\alpha - s_{bj}^\beta|$ can measure the degree of similarity between s_{ai}^α and s_{bj}^β . If the value of $|s_{ai}^\alpha - s_{bj}^\beta|$ is close to 0, the Euclidean distances s_{ai}^α and s_{bj}^β are deemed to be consistent; otherwise, s_{ai}^α and s_{bj}^β are deemed to be inconsistent. Using s_{ai}^α and s_{bj}^β to multiply $|s_{ai}^\alpha - s_{bj}^\beta|$ distinguishes the influence of the CMNs on the degree of distance consistency. The closer the Euclidean distance of an unmatched node and its CMN, the greater the influence of this CMN. $(s_{ai}^\alpha \cdot |s_{ai}^\alpha - s_{bj}^\beta| \cdot s_{bj}^\beta)$ can be transformed by the sigmoid function to ensure that its value is between 0 and 1. In addition, for an unmatched node pair, the larger the value of $|s_{ai}^\alpha - s_{bj}^\beta|$, the smaller the distance consistency should be, which is reflected by the exponential function $\exp(-(\cdot))$ in the formula.

In summary, the degree of distance consistency has the following characteristics:

- (i) the greater the number of CMNs, the greater the degree of distance consistency;
- (ii) the smaller the Euclidean distance between an unmatched node and its CMN, the greater the influence of this CMN on the degree of distance consistency;
- (iii) the smaller the difference between two Euclidean distances formed by unmatched nodes across different layers and their CMNs, the larger the degree of distance consistency.

4.4. Prediction

After obtaining the degrees of vector consistency and distance consistency for unmatched node pair (u_a^α, u_b^β) , we associate these two types of consistency to calculate the final degree of match. The formula can be represented as

$$r(u_a^\alpha, u_b^\beta) = \delta \cdot p(u_a^\alpha, u_b^\beta) + (1 - \delta) \cdot q(u_a^\alpha, u_b^\beta), \quad (12)$$

where δ is a control parameter that takes a value from 0 to 1. If $\delta = 0$, the degree of match is only related to the distance consistency, whereas if $\delta = 1$, the degree of match is only related to the vector consistency.

For any node u_a^α in layer α , we can calculate its degree of match with all unmatched nodes in layer β . We can then predict an interlayer link by identifying the counterpart node in layer β that has the highest degree of match with node u_a^α or offer a list of nodes in layer β as potential counterparts of node u_a^α .

4.5. Optimization

To reduce the time complexity, we optimized the calculation of the degrees of vector consistency and distance consistency.

4.5.1. Optimization of vector consistency calculation

The degree of vector consistency for each unmatched node pair can be calculated using Eq. (10). However, many calculations are repeated, such as that of $\|\mathbf{u}_b^\beta\|$. We propose an approach based on a matrix operation to reduce the computational time complexity.

For all unmatched nodes, denoting $\mathbf{B}^\alpha = [\mathbf{u}_1^\alpha, \mathbf{u}_2^\alpha, \dots, \mathbf{u}_{n^\alpha-n}^\alpha]$, $\mathbf{B}^\beta = [\mathbf{u}_1^\beta, \mathbf{u}_2^\beta, \dots, \mathbf{u}_{n^\beta-n}^\beta]$, $\phi(\mathbf{B}^\alpha) = [\phi(\mathbf{u}_1^\alpha), \phi(\mathbf{u}_2^\alpha), \dots, \phi(\mathbf{u}_{n^\alpha-n}^\alpha)]$, $\mathbf{b}^\alpha = [\|\mathbf{u}_1^\alpha\|, \|\mathbf{u}_2^\alpha\|, \dots, \|\mathbf{u}_{n^\alpha-n}^\alpha\|]^\text{T}$,

$\mathbf{b}^\beta = [\|\mathbf{u}_1^\beta\|, \|\mathbf{u}_2^\beta\|, \dots, \|\mathbf{u}_{n^\beta-n}^\beta\|]^\text{T}$, and $\phi(\mathbf{b}^\alpha) = [\|\phi(\mathbf{u}_1^\alpha)\|, \|\phi(\mathbf{u}_2^\alpha)\|, \dots, \|\phi(\mathbf{u}_{n^\alpha-n}^\alpha)\|]^\text{T}$, the degree of vector consistency for all unmatched node pairs can be expressed as

$$\mathbf{P} = \frac{\phi(\mathbf{B}^\alpha)^\text{T} \cdot \mathbf{B}^\beta}{\phi(\mathbf{b}^\alpha)^\text{T} \cdot \mathbf{b}^\beta}. \quad (13)$$

4.5.2. Optimization of distance consistency calculation

If h_{ai-bj} is denoted by $\exp(-(s_{ai}^\alpha \cdot |s_{ai}^\alpha - s_{bj}^\beta| \cdot s_{bj}^\beta))$, it is clear that if interlayer node pair (v_i^α, v_j^β) is the CMN of unmatched node pair (u_a^α, u_b^β) , e_{ai}^α and e_{bj}^β will be equal to 1; thus, $e_{ai}^\alpha \cdot h_{ai-bj} \cdot e_{bj}^\beta = h_{ai-bj}$. In contrast, if interlayer node pair (v_i^α, v_j^β) is not the CMN of unmatched node pair (u_a^α, u_b^β) , e_{ai}^α or e_{bj}^β will be equal to 0; thus, $e_{ai}^\alpha \cdot h_{ai-bj} \cdot e_{bj}^\beta = 0$. Therefore, Eq. (11) can be rewritten as

$$q(u_a^\alpha, u_b^\beta) = \sum_{\forall (v_i^\alpha, v_j^\beta) \in \Phi} e_{ai}^\alpha \cdot h_{ai-bj} \cdot e_{bj}^\beta. \quad (14)$$

If node v_i^α is an a priori interlayer node in layer α , a counterpart node must exist in layer β , and vice versa. Based on this, we can make the a priori interlayer nodes uniform, as follows: $(v_1^\alpha, v_1^\beta), \dots, (v_i^\alpha, v_i^\beta), \dots, (v_n^\alpha, v_n^\beta)$. Therefore, Eq. (14) can be replaced with

$$q(u_a^\alpha, u_b^\beta) = \sum_{i=1}^n e_{ai}^\alpha \cdot h_{ai-bi} \cdot e_{bi}^\beta. \quad (15)$$

Using the vector form, Eq. (15) can be replaced by

$$q(u_a^\alpha, u_b^\beta) = [e_{a1}^\alpha, \dots, e_{ai}^\alpha, \dots, e_{an}^\alpha] \cdot \begin{bmatrix} h_{a1-b1} \cdot e_{b1}^\beta \\ \vdots \\ h_{ai-bi} \cdot e_{bi}^\beta \\ \vdots \\ h_{an-bn} \cdot e_{bn}^\beta \end{bmatrix}. \quad (16)$$

We can use the Hadamard product to rewrite $[h_{a1-b1} \cdot e_{b1}^\beta, \dots, h_{ai-bi} \cdot e_{bi}^\beta, \dots, h_{an-bn} \cdot e_{bn}^\beta]^\text{T}$ as $[h_{a1-b1}, \dots, h_{ai-bi}, \dots, h_{an-bn}]^\text{T} \circ [e_{b1}^\beta, \dots, e_{bi}^\beta, \dots, e_{bn}^\beta]^\text{T}$. By denoting $\mathbf{h}_{ab} = [h_{a1-b1}, \dots, h_{ai-bi}, \dots, h_{an-bn}]^\text{T}$, $\mathbf{e}_a^\alpha = [e_{a1}^\alpha, \dots, e_{ai}^\alpha, \dots, e_{an}^\alpha]^\text{T}$, $\mathbf{e}_b^\beta = [e_{b1}^\beta, \dots, e_{bi}^\beta, \dots, e_{bn}^\beta]^\text{T}$, Eq. (16) can be rewritten as

$$q(u_a^\alpha, u_b^\beta) = (\mathbf{e}_a^\alpha)^\text{T} \cdot (\mathbf{h}_{ab} \circ \mathbf{e}_b^\beta). \quad (17)$$

By using Eq. (17), the degree of distance consistency for unmatched node pair (u_a^α, u_b^β) can be represented in vector operation form. Then, if we want to obtain the degree of distance consistency between node u_a^α and all the unmatched nodes in layer β , we can express Eq. (17) in matrix operation form. In a similar manner, we denote $\mathbf{H} = [\mathbf{h}_{a1}, \dots, \mathbf{h}_{ab}, \dots, \mathbf{h}_{an^\beta}]$, $\mathbf{E}^\beta = [\mathbf{e}_1^\beta, \dots, \mathbf{e}_b^\beta, \dots, \mathbf{e}_{n^\beta}^\beta]$. The degree of distance consistency between node u_a^α and all the unmatched nodes in layer β can be calculated as follows:

$$\mathbf{q}_a^\alpha = ((\mathbf{e}_a^\alpha)^T \cdot (\mathbf{H} \circ \mathbf{E}^\beta))^T. \quad (18)$$

By denoting $\mathbf{s}_a^\alpha = [s_{a1}^\alpha, \dots, s_{ai}^\alpha, \dots, s_{an}^\alpha]$, $\mathbf{s}_b^\beta = [s_{b1}^\beta, \dots, s_{bi}^\beta, \dots, s_{bn}^\beta]^T$, $\mathbf{S}^\beta = [\mathbf{s}_1^\beta, \dots, \mathbf{s}_b^\beta, \dots, \mathbf{s}_{n^\beta}^\beta]^T$, matrix \mathbf{H} can be calculated as

$$\mathbf{H} = \exp\{(\mathbf{i} \cdot \mathbf{s}_a^\alpha) \circ |\mathbf{i} \cdot \mathbf{s}_a^\alpha - \mathbf{S}^\beta| \circ \mathbf{S}^\beta\}, \quad (19)$$

where \mathbf{i} is a column vector with n^β elements. The value of each element in vector \mathbf{i} is 1.

By joining the vector for the degree of distance consistency for all unmatched nodes in layer α , we can obtain the matrix for the degree of distance consistency for all unmatched node pairs, which can be represented as $\mathbf{Q} = [\mathbf{q}_1^\alpha, \dots, \mathbf{q}_a^\alpha, \dots, \mathbf{q}_{n^\alpha}^\alpha]^T$.

Table 2: Statistics of Datasets. $|V|$ and $|E|$ are the number of nodes and intralayer links respectively. k_{max} is the maximum degree, $\langle k \rangle$ is the average degree, r is the degree-degree correlation, c is the clustering coefficient, H is the degree heterogeneity, as $H = \langle k^2 \rangle / \langle k \rangle^2$, and $|E^{\alpha\beta}|$ is the number of interlayer links.

Network	$ V $	$ E $	k_{max}	$\langle k \rangle$	r	c	H	$ E^{\alpha\beta} $
Foursquare	5,313	76,972	552	20.42	-0.193	0.23	3.446	3,148
Twitter	5,120	164,920	1725	51.01	-0.214	0.30	4.489	
DBLP_DataMining	11,526	47,326	117	36.68	0.110	0.85	2.176	1,295
DBLP_MachineLearning	12,311	43,948	552	20.42	-0.193	0.23	3.446	

Finally, the matrix for the degree of match for all unmatched node pairs can be obtained by

$$\mathbf{R} = \delta \cdot \mathbf{P} + (1 - \delta) \cdot \mathbf{Q}. \quad (20)$$

The interlayer link prediction results are obtained by ranking each row or column of \mathbf{R} in reverse order according to the degree of match.

5. Experiments

In this section, we first describe the datasets, baselines, and evaluation metrics. We then compare the proposed framework with baseline methods on two real-world datasets.

5.1. Datasets

To evaluate the performance of our proposed framework and baseline methods, we used the following two real-world multiplex network datasets in our experiments (cf. Table 2):

- **Foursquare–Twitter (FT)**: This dataset was collected from Foursquare and Twitter by Zhang et al. [59]. The ground truth for this dataset is provided in Foursquare’s profiles, and the nodes of the two social networks are partially aligned.
- **DBLP_DataMining-DBLP_MachineLearning (DBLP)**: This dataset was collected from the Citation Network Dataset³ [79] and processed by Liu et al. [71]. It is a co-authored multiplex network, one layer of which consists of researchers who published articles in journals or conference proceedings related to data mining, and the other layer containing researchers who published articles in journals or conference proceedings related to machine learning. The ground truth was obtained by collecting the authors who published articles in both fields.

5.2. Comparison Methods

We used several state-of-the-arts as baselines, which are as follows.

- **DeepLink [33]**: DeepLink is a semi-supervised learning algorithm that leverages traditional random walks to generate social sequences for the network embedding and utilizes the duality of mapping to improve the prediction performance.
- **IONE [32]**: Input–output network embedding (IONE) projects multiple social networks into a common embedded space and matches same-user accounts by calculating the cosine similarity between the vectors of two nodes. In IONE, it represents each account by three vectors: a node vector, an input context vector, and an output context vector.

³<https://www.aminer.cn/citation>

- **ONE** [32]: This method is a simplified version of IONE. In this method, an account is represented by two vectors: a node vector and an output context vector.
- **IONE-D** [71]: This method is a refined version of IONE that explores the community structure of the SMNs and incorporates the structural diversity to characterize a set of interlayer links.
- **BootEA** [80]: This is a bootstrapping approach that aligns the entities of different knowledge graphs based on network embedding. It iteratively labels potential entity pairs as training data to overcome the lack of a sufficiently large training set and leverages an editing method to reduce error accumulation during the iterations.
- **PALE** [31]: This method projects each SMN into a unique low-dimensional space and represents nodes by low-dimensional vectors in a latent space. Then, it learns a cross-layer mapping function for predicting interlayer links.
- **MAH** [70]: Manifold alignment on hypergraph (MAH) tries to map common users across SMNs based on the network embedding method. It adopts a hypergraph to model high-order relations of SMNs and represents nodes into a common latent space. It infers correspondence by comparing distances between the vectors of the unmatched nodes.
- **MAG** [70]: Manifold alignment on traditional graphs (MAG) is a method that uses $w(u_i, u_j) = |R_{u_i} \cap R_{u_j}| / (|R_{u_i}| + |R_{u_j}|)$ for the calculation of node-to-node pairwise weights to build a graph for each SMN. The method for obtaining the node ranking result is the same as that for MAH.
- **CRW** [59]: Collective random walk (CRW) is a joint link fusion approach for predicting the intralayer links and interlayer links simultaneously; it transfers information relating to intralayer links from one layer to another.

5.3. Experiment Configuration

We employed *Precision@N* ($P@N$) [32, 3] and *MAP* [3] as the metrics to evaluate the performance of all methods. $P@N$ is defined as

$$P@N = \sum_{i=1}^m \mathbb{1}_i\{\text{success@N}\}/m, \quad (21)$$

where $\mathbb{1}_i\{\text{success@N}\}$ indicates whether the correct interlayer link exists in the top- N list, and m represents the number of all unobserved interlayer links. It is noteworthy that *Precision@N* is actually the same as *Recall@N* and *F1@N* in the field of interlayer link prediction because *Precision@N* represents the true positive prediction rate. When $N = 1$, $P@1$ equates to the metric of precision.

MAP is used to evaluate the ranked performance of different methods and is defined as

$$MAP = (\sum_{i=1}^n \frac{1}{r_i})/m, \quad (22)$$

where r_i represents the rank of the i th unmatched interlayer link. The higher the values of $P@N$ and *MAP*, the better the performance of the method.

To test the performance, the set of all interlayer links was randomly divided into two parts for each experiment (i) a training set Φ , which was treated as the set of a priori interlayer links; and (ii) a test set Ψ , which was used for testing and can be considered a collection of the unmatched node pairs waiting for prediction. The ratio of the size of the training set to the size of the set of all interlayer links is called the training ratio, which we varied in some of the experiments. Our task was to uncover the interlayer links in the test set based on the information in the training set and each layer of the multiplex network. For all experiments, we set the control parameter δ to 0.9 for the FT dataset and to 0.4 for the DBLP dataset (as determined in preliminary experiments). The results of these experiments are displayed in Table 3. Each of the experiments was repeated ten times, and the average values were taken as the results.

5.4. Experimental Results

In this subsection, we report a comparison of the results of the baseline methods and the proposed method for different $@N$ settings, training ratios, dimensionalities, and numbers of iterations. We also compare the performance of the proposed embedding method with two state-of-the-art embedding methods, including DeepWalk [63] and node2vec [64].

Table 3: Performance of MulCEV on different δ , where 1st column is metric, 2nd column is datasets, 3rd column is training ratios.

		δ										
		0.0	0.1	0.2	0.3	0.4	0.5	0.6	0.7	0.8	0.9	
$P@30$	FT	0.3	0.4224	0.4407	0.4471	0.4546	0.4614	0.4710	0.4869	0.5036	0.5151	0.5155
		0.6	0.5285	0.5337	0.5388	0.5425	0.5506	0.5594	0.5741	0.5925	0.6124	0.6168
		0.9	0.6025	0.6047	0.6110	0.6160	0.6167	0.6308	0.6450	0.6649	0.6902	0.6959
	DBLP	0.3	0.2407	0.2413	0.2416	0.2418	0.2419	0.2418	0.2366	0.2255	0.2143	0.2043
		0.6	0.3782	0.3796	0.3796	0.3796	0.3796	0.3809	0.3649	0.3328	0.3087	0.2900
		0.9	0.5152	0.5152	0.5152	0.5152	0.5291	0.5152	0.4943	0.4456	0.3759	0.2785

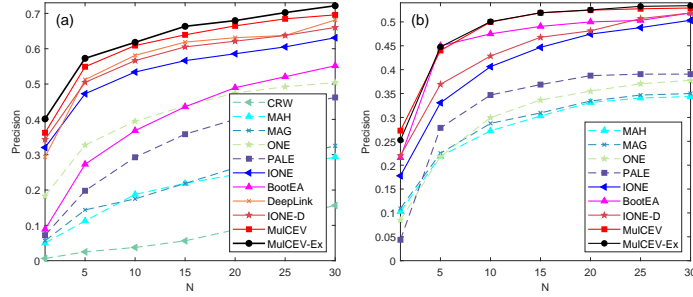


Figure 4: Comparison between baselines and our proposed methods for different @N settings. (a) *Precision* of different @N settings on the dataset FT, (b) *Precision* of different N settings on the dataset DBLP.

5.4.1. Performance with different @N settings

We first evaluate the performance of the baseline methods and the proposed method at different @N settings. In the proposed framework, the first step is cross-layer extension. This step, however, is not mandatory. We call the version without cross-network extension MulCEV, and the version with cross-network extension MulCEV-Ex.

Referring to Refs. [71] and [33], we set 90.0% of the interlayer links as the training set and the rest as the test set. Figure 4 displays the precision of the baseline methods and the proposed method under this setting. From the figure, we can see that MulCEV-Ex achieved the highest precision for all @N settings. On the FT dataset, the precision increased by a maximum of 10.8% and an average of 5.8% over DeepLink, the best of the baseline methods. On the DBLP dataset, the precision increased by a maximum of

Table 4: *MAP* of different methods.

Datasets	Methods						
	MulCEV-Ex	MulCEV	IONE-D	BootEA	IONE	PALE	ONE
FT	0.4808	0.4511	0.4228	0.2251	0.4005	0.1420	0.2563
DBLP	0.3651	0.3520	0.2979	0.3487	0.2578	0.1516	0.1075

3.7% and an average of 2.3% over BootEA. MulCEV achieved the second-highest performance, for a maximum increase of 6.8% and 5.7% on the two respective datasets compared with the best of the baseline methods. In contrast with other methods based on network embedding, our method further considers distance consistency with CMNs. The results imply that the distance consistency provides more clues and better facilitates the prediction of interlayer links. MulCEV-Ex was better than MulCEV under most settings because MulCEV-Ex leverages a priori interlayer links to extend each layer of the multiplex network. The extended layer has more edges to guide the embedding than the non-extended network so that the node positions in the embedding space can better reflect the relationships between nodes. Such advantages are highlighted in the subsequent matching process. The improvement of MulCEV-Ex over MulCEV was greater on the FT dataset than on the DBLP dataset, as the percentage of interlayer nodes is greater in the FT dataset than in the DBLP dataset. The greater the number of interlayer links, the greater the number of intralayer links that can be extended.

CRW was the lowest-precision method, showing that the traditional link-based prediction method is not as accurate as the network embedding approach. MAH and MAG showed better performance than CRW but were a bit worse than the other methods. This may be because MAH needs hypergraph information, which is often difficult to obtain for an actual SMN and thus must be built using specific methods based on the data obtained, leading to poor performance by MAH. MAG uses a formula for the calculation of node-to-node pairwise weights to build a graph for each SMN and obtains ranking results by the same method as MAH, so its performance is similar to MAH's.

With regard to IONE and its two variants ONE and IONE-D, ONE does not consider the information of the input context of the node, and its performance was not as good as that of IONE. IONE-D, although based on IONE, further considers the impact of community-based structural diversity, and

so it exhibited better performance than IONE. PALE does not consider the input and output contexts of the node separately; its performance was not as good as IONE’s. It is noteworthy that IONE and PALE are two classical methods based on network embedding; IONE embeds all layers into a common latent space, and PALE embeds each layer into a unique space. On the two datasets, MulCEV increased the precision by an average of 7.0% and 6.8%, respectively, over IONE and an average of 28.4% and 15.8%, respectively, over PALE.

Compared with other methods, BootEA showed superior performance on the DBLP dataset but worse performance on the FT dataset. This may be because during the process of predicting interlayer links, BootEA iteratively labels potential node pairs as training data to overcome the lack of a sufficiently large training set. The percentage of interlayer nodes in the DBLP dataset is smaller than that in the FT dataset. Through automatic labeling, more training data are provided in the DBLP dataset, thereby allowing the advantages of BootEA to be better reflected. DeepLink gave the best performance of the baselines because it utilizes dual learning for the pretraining of the mapping function.

With all methods, we observe that as N increases, the precision of the various methods also increases. This is because @ N denotes the number of potential matches recommended by different methods for each unmatched node. The greater the value of N , the higher the number of candidate matches and the higher the probability of success in finding the correct match.

We also investigated the ranking performance of our suggested methods and some baselines with the 90.0% training ratio; Table 4 shows the results. The highest value for each dataset is in boldface. We can see that MulCEV-Ex outperformed all the comparison methods, and MulCEV was better than all the baseline methods. This observation further demonstrates the effectiveness and merits of the proposed framework.

It is worth noting that of all the methods, MulCEV-Ex is the only one that extends the intralayer links by interlayer links. Therefore, in order to conduct the comparison of the different methods under the same conditions to the extent possible, in the subsequent experiments we excluded MulCEV-Ex and used only MulCEV for the comparisons with the baselines.

5.4.2. *Effect of training ratio*

We evaluated the performance of the baselines and MulCEV under different settings for the training ratio. We set training ratios of 10% to 90% in

10% increments; $N = 30$. Figure 5 displays the $P@30$ of the baselines and MulCEV under these settings.

From the figure, we can see that the proportion of interlayer links used for training markedly affected the performance of all of the methods. For each method, $P@30$ increased with the training ratio. This is because the greater the training ratio, the greater the quantity of training data. For the methods that embed each layer into a unique latent space, there are more inputs to learn the mapping function; for the method embedding all layers into a common latent space, there are more inputs to align nodes to the common embedding space. Moreover, the rankings of the performance of all methods on the two datasets are similar to those under various $@N$ settings. The reasons are the same as those illustrated in Fig. 4. In particular, MulCEV achieved the highest precision for almost all training ratios. On the FT dataset, $P@30$ increased by a maximum of 4.8% and an average of 0.8% over DeepLink, the best of the baseline methods. On DBLP, it increased by a maximum of 1.0% and an average of 0.4% over the best baseline, IONE-D. These observations demonstrate the effectiveness and merits of the proposed method.

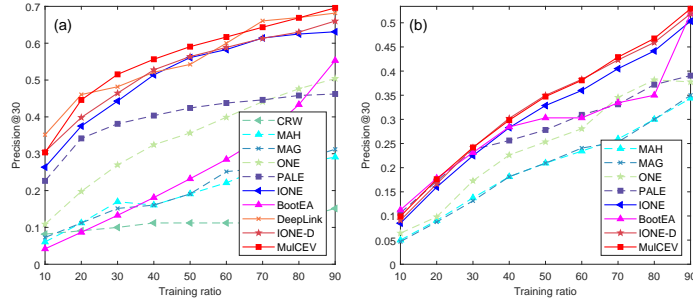


Figure 5: Comparison between baselines and MulCEV for different training ratios. (a) $P@30$ of different training ratios on the dataset FT, (b) $P@30$ of different training ratios on the dataset DBLP.

5.4.3. Effect of embedding dimensionality

We also evaluated the performance of the network embedding learning-based baseline methods and MulCEV using representations of different dimensionalities d . We set d to 16, 32, 64, 128, and 256; the training ratio was 90.0%, and $N = 30$. Figure 6 displays the $P@30$ values for the baselines and MulCEV under these settings.

From Fig. 6, we can see that the rankings of the performance of all methods on the two datasets are similar to the rankings under various $@N$ settings. The reasons are the same as those illustrated in Fig. 4. In particular, MulCEV achieved the highest precision for almost all dimensionalities. On the FT dataset, $P@30$ increased by a maximum of 8.2% and an average of 4.0% over DeepLink, the best of the baseline methods. On DBLP, it increased by a maximum of 2.3% and an average of 1.6% over the best baseline, BootEA. These observations demonstrate the effectiveness and merits of the proposed framework. Moreover, we can see that MulCEV, DeepLink, IONE-D, and IONE achieved their best performance on the FT dataset with $d = 128$, and on the DBLP dataset with $d = 64$. Other methods needed more dimensions to achieve their best performance. It is well known that the computational complexity of learning algorithms is highly dependent on the dimensionality of the embedding space: The lower the dimensionality, the lower the computational complexity. These results again demonstrate the effectiveness and merits of the proposed framework.

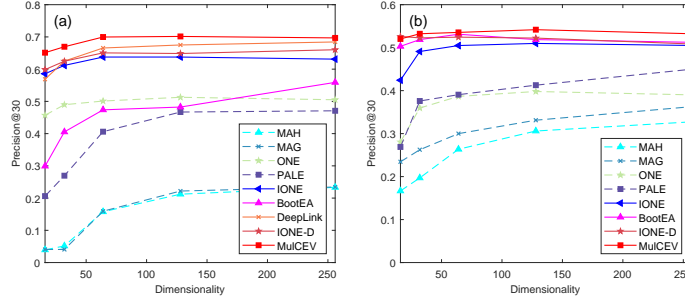


Figure 6: Comparison between baselines and MulCEV for different dimensionalities. (a) $P@30$ of different embedding dimensionality on the dataset FT, (b) $P@30$ of different embedding dimensionality on the dataset DBLP.

5.4.4. Effect of iteration count

The number of training iterations needed for a prediction method to converge is another important factor to consider in evaluating these methods. Referring to Refs. [71, 33], we set the training ratio to 90.0% and set $N = 30$ to execute the experiments for the evaluation of the baselines and MulCEV with different numbers of iterations. Figure 7 displays $P@30$ for the baselines and MulCEV under these settings.

From the figure, we can see that the rankings of the performance of all methods on the two datasets are similar to those under various @ N settings. The reasons are the same as those illustrated in Fig. 4. Meanwhile, MulCEV achieved the highest precision at almost all iteration counts. In particular, it achieved competitive results at very low training iteration counts; at 2000 iterations, it achieved $P@30$ values of 0.667 and 0.512 on the two respective datasets. In contrast, the $P@30$ values of all the baselines were close to zero. This is because the degree of match for MulCEV consists of two parts, degree of vector consistency and degree of distance consistency. The latter is calculated in advance (before the mapping function is learned) and provides some clues for making the predictions. Thereafter, the mapping function improves as the number of iterations increases, further improving the prediction performance.

DeepLink and PALE converged at similar iteration counts, around 10^5 . This is probably because these methods are based on similar concepts. They embed each layer of the multiplex network into a unique latent space and then use MLP to learn the mapping function and complete the matching. The convergent iteration counts for IONE and its two variant methods ONE and IONE-D are also similar, all of them converging between 10^6 and 10^7 . The reason is the same as that for DeepLink and PALE. Moreover, we can see that DeepLink and PALE converge to their best performance sooner than IONE and its variant methods. This is probably because IONE and its variants need to learn the context information for the nodes in each layer, and so they require a greater number of learning rounds to converge. $P@30$ for IONE and PALE would decrease at higher iteration counts because they incur overfitting problem.

5.4.5. *Effect of embedding method*

To evaluate the weighted-embedding method proposed in Section IV, we compared it with two commonly used network embedding methods: DeepWalk [63] and node2vec [64]. For DeepWalk, we set the number of walks per node to 20, the walk length to 80, and the window size to 5; for node2vec, we empirically set $q = 0.5$ and $p = 2$.

We compared the proposed weighted-embedding method and the comparison methods under various @ N settings and various training ratios on the FT dataset. Figure 8 displays the results. As can be seen in the figure, MulCEV achieved the highest precision at almost all @ N settings and training ratios. At the different @ N settings, $P@N$ increased by a maximum of 6.7%

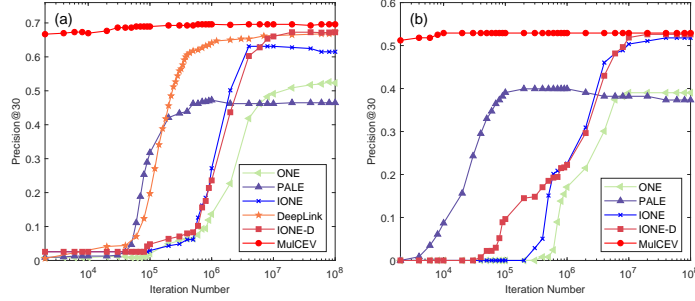


Figure 7: Comparison between baselines and MulCEV for different training iteration counts. (a) $P@30$ of different training iteration counts on the dataset FT, (b) $P@30$ of different training iteration counts on the dataset DBLP.

and an average of 2.9% over DeepWalk, the better of the two comparison embedding methods. At the different training ratios, $P@30$ increased by a maximum of 3.8% and an average of 2.7% over node2vec, the better of the two comparison embedding methods. These observations demonstrate the effectiveness and merits of the proposed weighted-embedding method.

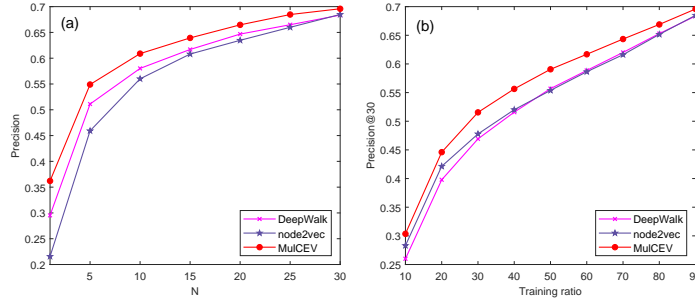


Figure 8: Comparison of different embedding methods. (a) Precision of different @N settings on the dataset FT, (b) $P@30$ of different training ratios on the dataset FT.

6. Conclusion

We have proposed a framework called MulCEV to predict the interlayer links in a multiplex network. This framework makes full use of the information in the latent representation space through vector consistency and distance consistency. Distance consistency leverages CMNs of the unmatched

nodes across different layers as references to provide additional clues for inter-layer link prediction. In addition, we modeled the layers as weighted graphs to obtain better representation for network embedding so that the higher the strength of the nodes' relationships, the more similar their embedding vectors in the latent representation space. To reduce the time complexity, we adopted matrix multiplication to optimize the process for calculating the degree of match. Experiments on two real-world multiplex network datasets demonstrated that the proposed MulCEV framework markedly outperforms several state-of-the-art methods.

In summary, the proposed framework further improves the accuracy of the network-based embedding method for dealing with interlayer link prediction, especially when the number of training iterations is low. The framework can effectively associate the accounts belonging to the same user across different SMNs solely by leveraging network structure attributes in the absence of attribute information such as username, age, or published content. Such an association can be used to establish patterns of law violations by cybercriminals, improve the understanding of information diffusion across SMNs, and provide support for criminal investigations and evidence collection through SMNs. In the future, we plan to further explore more reasonable embedding methods to capture the network structure and make predictions in scenarios in which the number of nodes is dynamically increased.

7. Acknowledgments

This work was supported by the National Natural Science Foundation of China under Grant Nos. U19A2081, 81602935, 81773548, 61802270, and 61802271; the Fundamental Research Funds for the Central Universities under Grant No. SCU2020D038; the Sichuan Science and Technology Program under Grant No. 20YYJC4001.

References

- [1] D. Centola, "The spread of behavior in an online social network experiment," *Science*, vol. 329, no. 5996, pp. 1194–1197, Sept. 2010.
- [2] C. Shi, Y. Li, J. Zhang, Y. Sun, and P. S. Yu, "A survey of heterogeneous information network analysis," *IEEE Transactions on Knowledge and Data Engineering*, vol. 29, no. 1, pp. 17–37, Jan. 2017.

- [3] K. Shu, S. Wang, J. Tang, R. Zafarani, and H. Liu, “User identity linkage across online social networks: A review,” ACM SIGKDD Explorations Newsletter, vol. 18, no. 2, pp. 5–17, Mar. 2017.
- [4] P. R. Center, “Demographics of social media users and adoption in united states,” <https://www.pewresearch.org/internet/fact-sheet/social-media/>, accessed 1 May 2020.
- [5] C. I. N. I. Center, “The 45th china statistical report on internet development,” Office of the Central Leading Group for Cyberspace Affairs, 2020.
- [6] D. T. Nguyen, H. Zhang, S. Das, M. T. Thai, and T. N. Dinh, “Least cost influence in multiplex social networks: Model representation and analysis,” in Proceedings of the 13th IEEE International Conference on Data Mining, Dallas, TX, USA, Dec. 2013, pp. 567–576.
- [7] Y. Jiang and J. Jiang, “Understanding social networks from a multiagent perspective,” IEEE Transactions on Parallel and Distributed Systems, vol. 25, no. 10, pp. 2743–2759, Oct. 2014.
- [8] M. Kivela, A. Arenas, M. Barthelemy, J. P. Gleeson, Y. Moreno, and M. A. Porter, “Multilayer networks,” Journal of Complex Networks, vol. 2, no. 3, pp. 203–271, July 2014.
- [9] A. Dadlani, M. S. Kumar, M. G. Maddi, and K. Kim, “Mean-field dynamics of inter-switching memes competing over multiplex social networks,” IEEE Communications Letters, vol. 21, no. 5, pp. 967–970, May 2017.
- [10] J. Liu, X. Wu, J. Lü, and X. Wei, “Infection-probability-dependent interlayer interaction propagation processes in multiplex networks,” IEEE Transactions on Systems, Man, and Cybernetics: Systems, 2019.
- [11] J. Gao, S. V. Buldyrev, S. Havlin, and H. E. Stanley, “Robustness of a network of networks,” Physical Review Letters, vol. 107, no. 19, p. 195701, Nov. 2011.
- [12] W. Wang, Q.-H. Liu, J. Liang, Y. Hu, and T. Zhou, “Coevolution spreading in complex networks,” Physics Reports, vol. 820, pp. 1–51, Aug. 2019.

- [13] Y. Li, X. Wu, J.-a. Lu, and J. Lü, “Synchronizability of duplex networks,” IEEE Transactions on Circuits and Systems II: Express Briefs, vol. 63, no. 2, pp. 206–210, Feb. 2016.
- [14] F. C. Santos, M. D. Santos, and J. M. Pacheco, “Social diversity promotes the emergence of cooperation in public goods games,” Nature, vol. 454, no. 7201, pp. 213–216, July 2008.
- [15] R. Tang, S. Jiang, X. Chen, H. Wang, W. Wang, and W. Wang, “Interlayer link prediction in multiplex social networks: an iterative degree penalty algorithm,” Knowledge-Based Systems, vol. 194, p. 105598, Apr. 2020.
- [16] X. Kong, J. Zhang, and P. S. Yu, “Inferring anchor links across multiple heterogeneous social networks,” in Proceedings of the 22nd ACM International Conference on Information and Knowledge Management, San Francisco, CA, USA, Oct. 2013, pp. 179–188.
- [17] A. Cheng, C. Zhou, H. Yang, J. Wu, L. Li, J. Tan, and L. Guo, “Deep active learning for anchor user prediction,” in Proceedings of the 28th International Joint Conference on Artificial Intelligence, Macao, China, Aug. 2019, pp. 2151–2157.
- [18] S. Zhang, H. Tong, R. Maciejewski, and T. Eliassi-Rad, “Multilevel network alignment,” in Proceedings of the 28th International Conference on World Wide Web, San Francisco, CA, USA, May 2019, pp. 2344–2354.
- [19] X. Chu, X. Fan, D. Yao, Z. Zhu, J. Huang, and J. Bi, “Cross-network embedding for multi-network alignment,” in Proceedings of the 28th International Conference on World Wide Web, San Francisco, CA, USA, May 2019, pp. 273–284.
- [20] C. Li, S. Wang, Y. Wang, P. Yu, Y. Liang, Y. Liu, and Z. Li, “Adversarial learning for weakly-supervised social network alignment,” in Proceedings of the 33rd AAAI Conference on Artificial Intelligence, vol. 33, Honolulu, Hawaii, USA, Feb. 2019, pp. 996–1003.
- [21] J. Zhou and J. Fan, “Translink: User identity linkage across heterogeneous social networks via translating embeddings,” in Proceedings of

the 38th IEEE Conference on Computer Communications, Paris, France, Apr. 2019, pp. 2116–2124.

- [22] F. Zhou, Z. Wen, G. Trajcevski, K. Zhang, T. Zhong, and F. Liu, “Disentangled network alignment with matching explainability,” in Proceedings of the 38th IEEE Conference on Computer Communications, Paris, France, Apr. 2019, pp. 1360–1368.
- [23] R. Zafarani, L. Tang, and H. Liu, “User identification across social media,” ACM Transactions on Knowledge Discovery from Data, vol. 10, no. 2, pp. 1–30, Oct. 2015.
- [24] Y. Li, Z. Su, J. Yang, and C. Gao, “Exploiting similarities of user friendship networks across social networks for user identification,” Information Sciences, vol. 506, pp. 78–98, Jan. 2020.
- [25] X. Han, L. Wang, C. Cui, J. Ma, and S. Zhang, “Linking multiple online identities in criminal investigations: A spectral co-clustering framework,” IEEE Transactions on Information Forensics and Security, vol. 12, no. 9, pp. 2242–2255, Sept. 2017.
- [26] W. Li, S. Tang, W. Fang, Q. Guo, X. Zhang, and Z. Zheng, “How multiple social networks affect user awareness: The information diffusion process in multiplex networks,” Physical Review E, vol. 92, no. 4, p. 042810, Oct. 2015.
- [27] H. Arshad, A. Jantan, and E. Omolara, “Evidence collection and forensics on social networks: Research challenges and directions,” Digital Investigation, vol. 28, pp. 126–138, Mar. 2019.
- [28] X. Zhou, X. Liang, H. Zhang, and Y. Ma, “Cross-platform identification of anonymous identical users in multiple social media networks,” IEEE Transactions on Knowledge and Data Engineering, vol. 28, no. 2, pp. 411–424, Feb. 2016.
- [29] S. Fu, G. Wang, S. Xia, and L. Liu, “Deep multi-granularity graph embedding for user identity linkage across social networks,” Knowledge-Based Systems, vol. 193, p. 105301, Apr. 2020.

- [30] D. Zhang, J. Yin, X. Zhu, and C. Zhang, “Network representation learning: A survey,” IEEE transactions on Big Data, vol. 6, no. 1, pp. 3–28, Mar. 2020.
- [31] T. Man, H. Shen, S. Liu, X. Jin, and X. Cheng, “Predict anchor links across social networks via an embedding approach,” in Proceedings of the 25th International Joint Conference on Artificial Intelligence, vol. 16, New York, USA, July 2016, pp. 1823–1829.
- [32] L. Liu, W. K. Cheung, X. Li, and L. Liao, “Aligning users across social networks using network embedding,” in Proceedings of the 25th International Joint Conference on Artificial Intelligence, New York, USA, July 2016, pp. 1774–1780.
- [33] F. Zhou, L. Liu, K. Zhang, G. Trajcevski, J. Wu, and T. Zhong, “Deeplink: A deep learning approach for user identity linkage,” in Proceedings of the 37th IEEE Conference on Computer Communications, Honolulu, HI, USA, Apr. 2018, pp. 1313–1321.
- [34] X. Mu, F. Zhu, E.-P. Lim, J. Xiao, J. Wang, and Z.-H. Zhou, “User identity linkage by latent user space modelling,” in Proceedings of the 22nd ACM SIGKDD International Conference on Knowledge Discovery and Data Mining, San Francisco, CA, USA, Aug. 2016, pp. 1775–1784.
- [35] Y. Wang, H. Shen, J. Gao, and X. Cheng, “Learning binary hash codes for fast anchor link retrieval across networks,” in Proceedings of the 28th International Conference on World Wide Web, San Francisco, CA, USA, May 2019, pp. 3335–3341.
- [36] D. Zhao, N. Zheng, M. Xu, X. Yang, and J. Xu, “An improved user identification method across social networks via tagging behaviors,” in Proceedings of the 30th International Conference on Tools with Artificial Intelligence, Volos, Greece, Nov. 2018, pp. 616–622.
- [37] R. Zafarani and H. Liu, “Connecting corresponding identities across communities,” in Proceedings of the 3rd International Conference on Weblogs and Social Media, San Jose, California, USA, May 2009.
- [38] D. Perito, C. Castelluccia, M. A. Kaafar, and P. Manils, “How unique and traceable are usernames?” in Proceedings of the 11th International

Symposium on Privacy Enhancing Technologies Symposium, Waterloo, ON, Canada, July 2011, pp. 1–17.

- [39] R. Zafarani and H. Liu, “Connecting users across social media sites: a behavioral-modeling approach,” in Proceedings of the 19th ACM SIGKDD international conference on Knowledge discovery and data mining, Chicago, IL, USA, Aug. 2013, pp. 41–49.
- [40] J. Liu, F. Zhang, X. Song, Y.-I. Song, C.-Y. Lin, and H.-W. Hon, “What’s in a name? an unsupervised approach to link users across communities,” in Proceedings of the 6th ACM International Conference on Web Search and Data Mining, Rome, Italy, Feb. 2013, pp. 495–504.
- [41] Y. Li, Y. Peng, Z. Zhang, H. Yin, and Q. Xu, “Matching user accounts across social networks based on username and display name,” World Wide Web, vol. 22, no. 3, pp. 1075–1097, Apr. 2019.
- [42] F. Carmagnola and F. Cena, “User identification for cross-system personalisation,” Information Sciences, vol. 179, no. 1-2, pp. 16–32, Jan. 2009.
- [43] T. Iofciu, P. Fankhauser, F. Abel, and K. Bischoff, “Identifying users across social tagging systems,” in Proceedings of the 5th International Conference on Weblogs and Social Media, Barcelona, Catalonia, Spain, July 2011.
- [44] F. Abel, E. Herder, G.-J. Houben, N. Henze, and D. Krause, “Cross-system user modeling and personalization on the social web,” User Modeling and User-Adapted Interaction, vol. 23, no. 2-3, pp. 169–209, Nov. 2013.
- [45] O. Goga, D. Perito, H. Lei, R. Teixeira, and R. Sommer, “Large-scale correlation of accounts across social networks,” University of California at Berkeley, 2013.
- [46] K. Cortis, S. Scerri, I. Rivera, and S. Handschuh, “An ontology-based technique for online profile resolution,” in Proceedings of the 4th International Conference on Social Informatics, Kyoto, Japan, Nov. 2013, pp. 284–298.

- [47] C. Riederer, Y. Kim, A. Chaintreau, N. Korula, and S. Lattanzi, “Linking users across domains with location data: Theory and validation,” in Proceedings of the 25th International Conference on World Wide Web, Montreal, Canada, Apr. 2016, pp. 707–719.
- [48] W. Chen, H. Yin, W. Wang, L. Zhao, and X. Zhou, “Effective and efficient user account linkage across location based social networks,” in Proceedings of the 34th IEEE International Conference on Data Engineering, Paris, France, Apr. 2018, pp. 1085–1096.
- [49] J. Feng, M. Zhang, H. Wang, Z. Yang, C. Zhang, Y. Li, and D. Jin, “Dplink: User identity linkage via deep neural network from heterogeneous mobility data,” in Proceedings of the 28th International Conference on World Wide Web, San Francisco, CA, USA, May 2019, pp. 459–469.
- [50] R. Zheng, J. Li, H. Chen, and Z. Huang, “A framework for authorship identification of online messages: Writing-style features and classification techniques,” Journal of the American Society for Information Science and Technology, vol. 57, no. 3, pp. 378–393, Feb. 2006.
- [51] A. Narayanan, H. Paskov, N. Z. Gong, J. Bethencourt, E. Stefanov, E. C. R. Shin, and D. Song, “On the feasibility of internet-scale author identification,” in Proceedings of the 33rd IEEE Symposium on Security and Privacy, San Francisco, California, USA, May 2012, pp. 300–314.
- [52] O. Goga, H. Lei, S. H. K. Parthasarathi, G. Friedland, R. Sommer, and R. Teixeira, “Exploiting innocuous activity for correlating users across sites,” in Proceedings of the 22nd international conference on World Wide Web, Rio de Janeiro, Brazil, May 2013, pp. 447–458.
- [53] A. Narayanan and V. Shmatikov, “De-anonymizing social networks,” in Proceedings of the 30th IEEE Symposium on Security and Privacy, Oakland, California, USA, May 2009, pp. 173–187.
- [54] N. Korula and S. Lattanzi, “An efficient reconciliation algorithm for social networks,” Proceedings of the VLDB Endowment, vol. 7, no. 5, pp. 377–388, Jan. 2014.
- [55] Y. Ren, C. C. Aggarwal, and J. Zhang, “Meta diagram based active social networks alignment,” in Proceedings of the 35th IEEE International

- Conference on Data Engineering, Macau, China, Apr. 2019, pp. 1690–1693.
- [56] Y. Zhu, L. Qin, J. X. Yu, Y. Ke, and X. Lin, “High efficiency and quality: large graphs matching,” The International Journal on Very Large Data Bases, vol. 22, no. 3, pp. 345–368, Sept. 2012.
 - [57] Y. Zhang, J. Tang, Z. Yang, J. Pei, and P. S. Yu, “Cosnet: Connecting heterogeneous social networks with local and global consistency,” in Proceedings of the 21st ACM SIGKDD International Conference on Knowledge Discovery and Data Mining, Sydney, NSW, Australia, Aug. 2015, pp. 1485–1494.
 - [58] J. Zhang and S. Y. Philip, “Multiple anonymized social networks alignment,” in Proceedings of the 15th IEEE International Conference on Data Mining, Atlantic City, NJ, USA, Nov. 2015, pp. 599–608.
 - [59] —, “Integrated anchor and social link predictions across social networks,” in Proceedings of the 24th International Joint Conference on Artificial Intelligence, Buenos Aires, Argentina, July 2015, pp. 2215–2132.
 - [60] S. Zhang and H. Tong, “Final: Fast attributed network alignment,” in Proceedings of the 22nd ACM SIGKDD International Conference on Knowledge Discovery and Data Mining, San Francisco, CA, USA, Aug. 2016, pp. 1345–1354.
 - [61] S. Zhang, H. Tong, R. Maciejewski, and T. Eliassi-Rad, “Multilevel network alignment,” in Proceedings of the 28th International Conference on World Wide Web, San Francisco, CA, USA, May 2019, pp. 2344–2354.
 - [62] P. Cui, X. Wang, J. Pei, and W. Zhu, “A survey on network embedding,” IEEE Transactions on Knowledge and Data Engineering, vol. 31, no. 5, pp. 833–852, June 2018.
 - [63] B. Perozzi, R. Al-Rfou, and S. Skiena, “Deepwalk: Online learning of social representations,” in Proceedings of the 20th ACM SIGKDD International Conference on Knowledge Discovery and Data Mining, New York City, USA, Aug. 2014, pp. 701–710.

- [64] A. Grover and J. Leskovec, “node2vec: Scalable feature learning for networks,” in Proceedings of the 22nd ACM SIGKDD International Conference on Knowledge Discovery and Data Mining, San Francisco, CA, USA, Aug. 2016, pp. 855–864.
- [65] J. Tang, M. Qu, M. Wang, M. Zhang, J. Yan, and Q. Mei, “Line: Large-scale information network embedding,” in Proceedings of the 24th International Conference on World Wide Web, Florence, Italy, May 2015, pp. 1067–1077.
- [66] X. Wang, P. Cui, J. Wang, J. Pei, W. Zhu, and S. Yang, “Community preserving network embedding,” in Proceedings of the 31st AAAI Conference on Artificial Intelligence, San Francisco, California, USA, Feb. 2017, pp. 203–209.
- [67] A. Zhiyuli, X. Liang, Y. Chen, and X. Du, “Modeling large-scale dynamic social networks via node embeddings,” IEEE Transactions on Knowledge and Data Engineering, vol. 31, no. 10, pp. 1994–2007, Oct. 2019.
- [68] L. Du, Y. Wang, G. Song, Z. Lu, and J. Wang, “Dynamic network embedding: An extended approach for skip-gram based network embedding,” in Proceedings of the 27th International Joint Conference on Artificial Intelligence, Stockholm, Sweden, July 2018, pp. 2086–2092.
- [69] R. Feng, Y. Yang, W. Hu, F. Wu, and Y. Zhang, “Representation learning for scale-free networks,” in Proceedings of the 32nd AAAI Conference on Artificial Intelligence, New Orleans, LA, USA, Feb. 2018, pp. 282–289.
- [70] S. Tan, Z. Guan, D. Cai, X. Qin, J. Bu, and C. Chen, “Mapping users across networks by manifold alignment on hypergraph,” in Proceedings of the 28th AAAI Conference on Artificial Intelligence, Québec City, Québec, Canada, Feb. 2014, pp. 159–165.
- [71] L. Liu, X. Li, W. Cheung, and L. Liao, “Structural representation learning for user alignment across social networks,” IEEE Transactions on Knowledge and Data Engineering, 2019.

- [72] X. Zhou, X. Liang, X. Du, and J. Zhao, “Structure based user identification across social networks,” IEEE Transactions on Knowledge and Data Engineering, vol. 30, no. 6, pp. 1178–1191, June 2018.
- [73] Y. Wang, C. Feng, L. Chen, H. Yin, C. Guo, and Y. Chu, “User identity linkage across social networks via linked heterogeneous network embedding,” World Wide Web, vol. 22, no. 6, pp. 2611–2632, Apr. 2019.
- [74] S. Wang, X. Li, Y. Ye, S. Feng, R. Y. Lau, X. Huang, and X. Du, “Anchor link prediction across attributed networks via network embedding,” Entropy, vol. 21, no. 3, p. 254, Mar. 2019.
- [75] M. Bayati, M. Gerritsen, D. F. Gleich, A. Saberi, and Y. Wang, “Algorithms for large, sparse network alignment problems,” in Proceedings of the 9th IEEE International Conference on Data Mining, Miami, FL, USA, Dec. 2009, pp. 705–710.
- [76] H. Cai, V. W. Zheng, and K. C.-C. Chang, “A comprehensive survey of graph embedding: Problems, techniques, and applications,” IEEE Transactions on Knowledge and Data Engineering, vol. 30, no. 9, pp. 1616–1637, Feb. 2018.
- [77] C. Manning and H. Schutze, Foundations of statistical natural language processing. London, England: MIT press, 1999.
- [78] B. W. SUTER, “The multilayer perceptron as an approximation to a bayes optimal discriminant function,” IEEE Transactions on Neural Networks, vol. 1, no. 4, pp. 296–298, Dec. 1990.
- [79] J. Tang, J. Zhang, L. Yao, and J. Li, “Extraction and mining of an academic social network,” in Proceedings of the 17th International Conference on World Wide Web, Beijing, China, Apr. 2008, pp. 1193–1194.
- [80] Z. Sun, W. Hu, Q. Zhang, and Y. Qu, “Bootstrapping entity alignment with knowledge graph embedding,” in Proceedings of the 27th International Joint Conference on Artificial Intelligence, Stockholm, Sweden, July 2018, pp. 4396–4402.